Enforced miR-144-5p Expression Sensitizes Erastin-Induced Ferroptosis via Targeting Nrf2 in Gastric Cancer Cells

Chuanliang Liu
WEIFANG PEOPLES' HOSPOTAL
Dan Wang
Weifang People's Hospital
Lei Li
Weifang People's Hospital
Ruihua Zhang (wfrmhospitalzrh@163.com)
Weifang People's Hospital https://orcid.org/0000-0001-8158-165X

Research

Keywords: miR-144-5p, erastin, ferroptosis, Nrf2, gastric cancer cells

Posted Date: January 21st, 2021

DOI: https://doi.org/10.21203/rs.3.rs-150859/v1

Abstract

Background: Ferroptosis is a newly described form of regulated cell death, targeting nuclear factor erythroid-2-related factor 2 (Nrf2) -mediated ferroptosis may be an attractive option to counteract malignant tumor. Whether miR-144-5p sensitize erastin-induced ferroptosis in gastric cancer via regulation of Nrf2 pathway is unclear.

Methods: To speculate the function of miR-144-5p in cancers, bioinformatic analysis was performed. Dual-luciferase reporter gene assay was used to predict effect of miR-144-5p on the expression of Nrf2. The expressions of miR-144-5p and Nrf2 in human gastric cancer cell lines and tissues were detected by qPCR, Immunohistochemistry or western blot.

Results: miR-144-5p, identified to wreck Nrf2 mRNA, was selected and overexpressed in gastric cancer cells to sensitize erastin-induced ferroptosis. Ectopic expression of miR-144-5p in AGS and BGC-823 cells downregulated the mRNA and protein expression of Nrf2. In addition, AGS and BGC-823 cell lines with exogenous expression of miR-144-5p were more sensitive to erastin-induced ferroptosis with overgeneration of lipid reactive oxygen species and depletion of glutathione.

Conclusions: miR-144-5p sensitizes erastin-induced ferroptosis via abrogating expression of Nrf2 to eliminate cancer cells selectively with high Nrf2 pathway activation.

1 Introduction

Ferroptosis, a form of regulated cell death characterized by the accumulation of lipid peroxides, is biochemically and genetically different from other kinds of programmed cell death, such as autophagy and apoptosis [1]. During this process, iron-dependent oxidase is initiated by the deficiency of glutathione (GSH)-dependent antioxidant defenses, leading to extensive lipid peroxidation and eventual cell death [1, 2]. Iron chelators or lipophilic antioxidants can impede ferroptosis [3].

Ferroptosis can be triggered by small molecules that inhibit glutamate/cystine antiporter (system Xc-), GSH biosynthesis, and GSH-dependent antioxidant enzymes, which contribute to the elimination of reactive oxygen species (ROS) [4, 5]. Erastin is selectively lethal to RAS-mutant oncogenic cells and triggers iron-dependent ferroptosis [3]. Moreover, it can induce ferroptosis in gastric cancer (GC) cells [6].

Erastin binds directly to voltage-dependent anion channel 2 and causes mitochondrial damage via overproduction of ROS in an NADH-dependent manner, leading to cell death in some tumor cells [5, 7]. In addition, it intensively enhances the therapeutic effect of cisplatin in wild-type EGFR cancer cells through inducing ROS-mediated caspase-independent cell death. Furthermore, erastin has the ability to decrease intracellular GSH concentration through directly depressing system Xc- activity with activation of the endoplasmic reticulum stress response, accelerating ROS accumulation during ferroptosis [5].

Nuclear factor erythroid-2-related factor 2 (Nrf2) is a redox-sensitive basic leucine zipper family transcription factor that transactivates cytoprotective pathways in response to oxidative stress. Its expression is high in many human tumors [8]. Recently, the aberrant activation of the Nrf2 pathway has been found to occur frequently in GC cell lines and tumor tissues [9]. The Nrf2 pathway senses and responds to changes in intracellular oxidative stress [10]. The Nrf2 signaling pathway plays a role in mediating lipid peroxidation and ferroptosis [11, 12], and high Nrf2 expression results in the insensitivity of cancer cells to ferroptosis induced by small molecules Therefore, blocking Nrf2 activity might be constructive in the treatment of GC patients whose tumors present Nrf2 pathway activation [13]. MiR-144-5p functions as a tumor suppressor by targeting Nrf2 [14, 15]. Here, we overexpressed miR-144-5p to knock down the expression of Nrf2 to sensitize erastin-induced ferroptosis in GC cells.

2 Materials And Methods

2.1 Cell culture and transfection

Human gastric cancer cell lines AGS and BGC-823 were obtained from the American Type Culture Collection (ATCC, VA, USA) and grown in Dulbecco's modified Eagles medium (DMEM; Thermo Fisher Scientific, MA, USA) supplemented with 10% fetal bovine serum (Gibco, NY, USA). AGS and BGC-823 cells were placed in 37 °C and 5% CO_2 humidified incubator. Gain and loss were performed to probe the effects of miR-144 in gastric cells. 40 nM hsa-miR-144 miRNA mimic and negative mimic control (mirVana™ miRNA mimic; Applied Biosystem) were used to increase miRNA activity. miR-144 inhibitor with 400 nM (anti-miR™ miRNA inhibitor; Applied Biosystem) was used for inhibition of miRNA activity. pcDNA3-EGFP-C4-Nrf2 plasmid was acquired from Addgene (Catalog: 21549; Cambridge, MA, USA). Lipofectamine 3000 was used for cell transfection according to the manufacturer's instructions (Invitrogen, Carlsbad, CA, USA).

2.2 Clinical samples

A total of 50 paired gastric cancer and adjacent normal tissues were retrospectively collected from Jan 2014 to Oct 2015 were pathologically diagnosed at Weifang Peoples' Hospital. All patients got primary gastric cancer and were undergone complete surgical resection, none of the patients received chemo- or radiotherapy prior to surgery. All samples were stored at − 80 °C before further processing. The study was approved by the Medical Ethics Committee of Weifang People's Hospital.

2.3 Bioinformatic analysis

To speculate the function of miR-144-5p in cancers, 10 microarrays (GSE118249, GSE115801, GSE106791, GSE66498, GSE56243, GSE45363, GSE45359, GSE28424, GSE28423, GSE19427) from Gene Expression Omnibus (GEO) (http://www.ncbi.nlm.ni h.gov/geo/) database were selected for analysis. When cancer cells were transfected with miR-144-5p, the expression differentiated genes with $P < 0.05$ and Log FC more than 0.5 or less than − 0.5 were selected, the date were analyzed with SangerBox software. To predicate the targeted gene of miR-144-5p and the miRNAs that modulate Nrf2,

MiRWALK2.0, TargetScan, PICTAR2 were used, genes projected by the servers were recognized as target genes.

2.4 Dual-Luciferase Reporter Gene Assay

Wild-type (WT) or mutant (Mut) 3’-untranslated regions (3’-UTRs) of Nrf2 were cloned into pGL3-Basic vectors (Promega, Madison, WI, USA) to construct pGL3/Nrf2-WT and pGL3/Nrf2-Mut recombinant vectors, respectively. Gastric cancer cells were inoculated in a 6-well cell plate, when the cell density reached 70% confluence. AGS cells cultured in 6-well plates were cotransfected with 100 nM miR-144-5p mimics and pGL3/ Nrf2-WT or pGL3/Nrf2-Mut with Lipofectamine 3000. Luciferase activity at 48 h after transfection was measured through the Dual-Luciferase report analysis system (Promega, Madison, WI, USA).

2.5 Cell viability assay and 5-Ethynyl-2’-deoxyuridine (EdU) assay

Cell viability was detected by MTT, 5×10^3 logarithmic phase AGS or BGC-823 cells were planted in 96-well plates per well and exposed to erastin (MedChemExpress, Shanghai, China) or bardoxolone methyl (BM, Nrf2 activator; MedChemExpress, Shanghai, China) for indicated times. Cells were incubated with MTT for 4 h, isopropanol was used to dissolve MTT formazan, and the absorbance of supernatant was measured at 490 nm using microplate reader (SpectraMax M5; Molecular Devices, CA, USA). To detect DNA synthesis and cell proliferation, 2.5×10^5 GC cells were seeded in a 6-well plate, EdU (25 μM, RiboBio, Guangzhou, China) was added for 4 h. 0.5% TritonX-100 was used to permeabilize and 4% formalin were applied to fix GC cells. Then Apollo reaction solution was added to stain the EdU for 30 min and Hoechst (Beyotime Biotechnology, Shanghai, China) to stain the nuclei.

2.6 Invasion assay

Cell invasion assay was carried out using Transwell inserts (Corning, NY, USA) with Matrigel® (BD Biosciences, CA, USA). Briefly, 5×10^4 AGS or BGC-823 cells in 100 μL serum-free medium were seeded in the upper chamber of the Transwell invasion system and the low chambers were filled with culture medium contained with 10% FBS as chemoattractant for 48 hours. Cells invaded into the lower chamber were fixed with methanol and stained with 0.1% crystal violet. Five low-magnification visual fields were randomly selected and the invasive cell numbers were counted. All experiments were performed in triplicate.

2.7 Quantitative polymerase chain reaction (qPCR)

TRIzol regent (Thermo Fisher Scientific, MA, USA) was used to extracted total RNA from GC cells. Single-stranded RNA is reverse transcribed into complementary DNA (cDNA) using QuantiTect Reverse Transcription Kit (Qiagen, CA, USA) according manufacturer's protocol, the entire reaction takes place at 42 °C for 15 minutes and is then inactivated at 95 °C. qPCR was performed to quantify the expression of miR-144-5p and Nrf2 mRNA in GC cells. 20 μL of each sample (100 ng total RNA) was used as template using SYBR-Green PCR Master Mix. The RNA expression levels were calculated as quantification cycle.

The primer sequences used for qPCR were: β-actin 5'-GGCACCCAGCACAATGAAG-3' (forward), and 5'-CGTCATACTCCTGCTTGCTG-3' (reverse); Nrf2 5'-ATAGCTGAGCCCAGTATC-3' (forward) and 5'-CATGCACGTGAGTGCTCT-3' (reverse); miR-144-5p 5'-TACAGTATAGATGATGTACT-3' (forward) and 5'-CAGTGCGTGTCGTGGAGT-3' (reverse); U6 5'-CTCGCTTCGGCAGCACA-3' (forward) and 5'-AACGCTTCACGAATTTGCGT-3' (reverse). Expressions of target genes were analyzed according to the $2^{-\Delta\Delta Ct}$ method.

2.8 Immunohistochemistry

5-μm-thick sections were used or immunohistochemistry assay. In brief, slides were dewaxed in xylene and then rehydrated in graded alcohols. Then the slides were treated with 3% hydrogen peroxide to block endogenous peroxidase and preincubated with a serum-free protein block solution to eliminate background stainfing. Slides were incubated with Nrf2 primary antibody overnight and were incubated with secondary antibody for 1 h at 37 °C. Reaction products were visualized with diaminobenzidine (DAB). Immunohistochemical staining results were evaluated by two independent pathologists who were blinded to the patients' clinicopathological details. The immunohistochemical staining was categorized on staining intensity and ratio of positive malignant cells. 0, no staining; 1, weak staining; 2, moderate staining; and 3, strong staining. In the case of ratio of positive malignant cells, 1, 0–25%; 2, 26–50%; 2, 51–75%; 4, more than 75%. For all patients, total scores from two parts were added together.

2.9 Western blotting

Cell proteins were extracted with RIPA lysis buffer and separated by 10% SDS-PAGE. The proteins were transferred to polyvinylidene difluoride membranes and blocked with 5% skim milk in TBST. The membranes incubated with anti-Nrf2 (dilution 1:500; catalog: ab31163; rabbit polyclonal; Abcam, MA, USA) at 4 °C overnight, the secondary antibody (dilution 1:500; rabbit monoclonal; Maxim, Fuzhou, China) treatment was applied for about 1 h at 37 °C. The immunoblots were measured by ECL (Pierce; Thermo Fisher Scientific, MA, USA). In addition, β-actin was used as an internal control (dilution 1:500; catalog: 0208; Beyotime Biotechnology, Haimen, China). The integrated density of the bands was quantified by ImageJ software (NIH, Bethesda, MD, USA).

2.10 ROS assay and Lipid peroxidation assessment

Cells were planted at 3×10^5 cells/well in 6-well plates, dichlorofluorescein diacetate (DCFH-DA) fluorescent probe detection kit (Thermo Fisher Scientific, MA, USA) was used to detect intracellular ROS level, results were monitored with fluorescence microscope and SpectraMax M5. Malondialdehy (MDA) assay kit (Jiancheng Bioengineering, Nanjing, China) was use to assess lipid peroxidation according to the manufacturer's instruction. The collected cells lyses were centrifuged to obtain the supernatant. 100 μL samples were added into 100 μL test solution at 95 ˚C for 40 min. After cooling down, the samples were centrifuged to get the supernatant, results was read in a microplate reader at 530 nm.

2.11 Measurement of intracellular GSH

The GSH assay kit (Beyotime Biotechnology, Nanjing, China) was used to analyze intracellular GSH levels. 5×10^6 AGS or BGC-823 cells were planted in 10 cm plates. After treatment with miR-144-5p mimic or inhibitor in the absence or presence of erastin for the indicated amount of time, cells were harvested by scratching and washed once with PBS. Then, cells were resuspended in MES-buffer (0.4 M 2-(N-mopholino) ethanesulphonic acid, 0.1 M phosphate, 2 mM EDTA, pH 6.0) and homogenized by sonification. Insoluble fragments were removed by centrifugation at 12,000 rpm for 10 min. The supernatant was used for intracellular GSH assay. GSH content was expressed as a ratio to the absorbance value at 412 nm of the control.

2.12 Statistical analysis

Data were analyzed using Prism 6.0 GraphPad software; the results are shown as mean ± SD or SEM. A one-way analysis of variance (ANOVA) was used for comparison among multiple groups, multiple comparison between the groups was performed using S-N-K method. Comparisons between two groups were performed using Student's t-test. Significant differences were defined as $P < 0.05$.

3 Results

3.1 MiR-144-5p plays an important role oxidized injury in cancer obtained through gene expression omnibus Microarrays

A total of 10 microarrays (GSE118249, GSE115801, GSE106791, GSE66498, GSE56243, GSE45363, GSE45359, GSE28424, GSE28423, GSE19427) from the GEO database met the entry criteria. Of these microarrays, miR-144-5p was downregulated in malignant tumor cells and tissues and regard as a tumor suppressor gene. In addition, with respect to the data from the tumor cell lines with or without overexpression of miR-144 (GSE118249), the differentiated genes with $P < 0.01$ and log FC more than 1 or less than − 1 were listed in Additional file 1: Table S1, in the total 95 genes, 12 genes were related with redox regulation (Fig. 1a, b).

3.2 miR-144-5p impaired expression of Nrf2 in GC cell

Nrf2, a basic leucine zipper protein, regulates the expression of antioxidant proteins that protect against oxidative damage triggered by injury. Nrf2 is identified as a putative target gene of miR-144-5p. To investigate whether miR-144-5p regulated endogenous Nrf2 expression in AGS or BGC-823 cell, Nrf2 expression was analyzed in AGS or BGC-823 cells following 48 h transfection with miR-144-5p mimic. The expression of Nrf2 mRNA (Fig. 2a, b) and protein (Fig. 2c-f) level was significantly decreased in AGS or BGC-823 cells compared to the control. On the contrary, expressions of Nrf2 mRNA and protein were significantly augmented in AGS or BGC-823 cells following transfection with anti miR-144-5p inhibitor (Fig. 2a-f).

3.3 Nrf2 is a potent target of miR-144-5p

Nrf2 plays an important role an important role against exogenous or endogenous oxidative stress to keep homeostasis of cell. Regarding the data from GSM3190202 and GSM1357599, Nrf2 is closely related with miR-144-5p (date not shown), so we wander that whether Nrf2 was a target of miR-144-5p. MiRWALK2.0 was mined to forecast the genes targeted by miR-144-5p, a total of 128 target genes were found, Nrf2 was one of the most important gene among them (Fig. 3a, Additional file 2: Table S2). With the help of TargetScan, 392 genes were predicated as the targeted gene of miR-144-5p, including Nrf2 (Additional file 3: Table S3). On the contrary, when Nrf2 was input for inquiry of miRNA, 17 miRNAs were displayed (Fig. 3b), and miR-144-5p is one the regulators for Nrf2 by targeting 303–313 of NEF2L2 3'UTR (Fig. 3c, d).

Clinically, gastric cancer sample were collected, the expressions of NRF2 and miR-144-5p were detected by qPCR, the relationship between Nrf2 and miR-144-5p were analyzed by logistic regression, and results showed that Nrf2 and miR-144-5p were related with each other (Fig. 3e). To probe the cross talk between Nrf2 and miR-144-5p, a dual luciferase report assay was performed, results showed that miR-144 mimic abrogated the intensity of luciferin of wild type, but not mutant type (Fig. 3f), indicating miR-144-5p targeted Nrf2 and post-transcriptionally regulated expression of Nrf2.

3.4 Association of miR-144-5p and Nrf2 with clinicopathological features

To make clear the clinical relevance of miR-144-5p expression in gastric cancer, the expressions of miR-144-5p were detected in a panel of 62 gastric cancer patients samples, and results showed that miR-144-5p was highly expressed in cancer tissues (Fig. 4a), and its expression was related with clinical stages (Fig. 4b). No significant correlation could be found between expression of miR-144-5p and age, gender and status of lymph node. Further, according to the median value of miR-144-5p in the gastric cancer tissues, the panel of 62 gastric cancer patients was divided into and miR-144-5p low-expression group miR-144-5p high-expression group. Kaplan-Meier test and log-rank test were performed to explore the relationship between miR-144-5p and prognosis of gastric cancer patients. The results demonstrated that breast cancer patients with high miR-144-5p expression showed significant longer 5-year overall survival (OS) compared with patients with low miR-144-5p expression (Fig. 4c). Moreover, the 5-year disease-free survival (DFS) for high miR-144-5p group was 7.1%, while was 23.8% for low miR-144-5p group (Fig. 4d). Receiver operating characteristic (ROC) curve methodology was used to assess the diagnostic utility of miR-144-5p for gastric cancers. The proportion under the ROC curve (AUC) was 0.68 (95% CI, 0.565–0.792, P = 0.014; Fig. 4e). In addition, the expression of Nrf2 in gastric cancer tissue and paracancerous tissue was detected by IHC (Fig. 4f); the expression of Nrf2 in cancer tissue was higher than paracancerous tissue (Fig. 4g), further, the highest expression of Nrf2 was found in gastric cancer patients with stage III and stage IV (Fig. 4h)

3.5 miR-144-5p inhibited cell proliferation and invasion in GC cells

To explore the role of miR-144-5p on cell in proliferation and invasion GC cells, miR-144-5p mimic was transfected into AGS or BGC-823 cells to enhance miR-144-5p expression or reduce its expression, which were confirmed by qPCR (Fig. 5a). MTT assay was performed to detect the ability of cell proliferation of transfected AGS or BGC-823 cells, and the results highlighted that proliferation of AGS or BGC-823 cells was suppressed by upregulation of miR-144-5p (Fig. 5b). On the contrary, downregulation of miR-144-5p advanced cell proliferation (Fig. 5c). In order to identify that miR-144-5p suppressed cell viability via modulating Nrf2, an exogenous Nrf2 was transfected into gastric cancer cells, exogenous Nrf2 showed protective effects against miR-144-5p as confirmed by MTT assay in AGS or BGC-823 cells (Fig. 5d, e). The impact of miR-144-5p on cell proliferation was further confirmed by EdU assay (Fig. 5f). Moreover, ectopic expression of miR-144-5p significantly arrested cell invasive ability confirmed by transwell assay; nevertheless, silence of miR-144-5p enhanced invasiveness of AGS and BGC-823 cells (Fig. 5g). Therefore, ectopic expression of miR-144-5p could suppress cell proliferation and invasion of GC cells.

3.6 miR-144-5p sensitized erastin-induced ferroptosis in GC cell

To investigate the role of miR-144-5p on sensitizing erastin-induced ferroptosis in AGS or BGC-823 cell, following 48 h transfection with miR-144-5p mimic or miR-144-5p inhibitor, the effect of miR-144-5p on the cell viability with or without erastin were examined by MTT assay. Results of cell viability showed that ectopic expression of miR-144-5p enhanced erastin-induced inhibition of proliferation in AGS or BGC-823 cells significantly compared with erastin (Fig. 6a); on the contrary, inhibition of miR-144-5p by inhibitor in AGS or BGC-823 cells rescued erastin-induced inhibition of proliferation (Fig. 6b). Cell death induced by ectopic miR-144-5p expression combined with erastin was significantly rescued by DFO (antioxidant trolox) or ferrostatin-1 (inhibitor of erastin-induced ferroptosis) in AGS or BGC-823 cells, respectively (Fig. 6c, d), but not Z-VAD-FMK (inhibitors of caspase), indicating that ectopic expression of miR-144-5p sensitizing erastin-induced iron-dependent ferroptosis in AGS cells but not apoptosis.

3.7 miR-144-5p enhanced erastin-induced overgeneration of lipid oxidation

Previous studies had proved that erastin-induced ferroptosis relied on overgeneration of ROS and MDA. Therefore, we measured generation of ROS and MDA in miR-144-5p overexpressed cell following treatment with erastin. At 8 h, ectopic expression of miR-144-5p and erastin resulted in overgeneration of ROS (Fig. 7a). Erastin alone displayed 264% and 163% increase in MDA generation in AGS or BGC-823 cells, respectively (Fig. 7b, c). MDA generation was obviously increased to 503% and 212% in gastric cancer cell treated with erastin (Fig. 7b, c). DFO effectively attenuated miR-144-5p and erastin-induced ROS production in AGS or BGC-823 cells (Fig. 7d).

Discussion

GC is one of the leading causes of cancer deaths worldwide, with 950,000 new cases being diagnosed yearly [16]. Patients with GC have poor prognosis, with median survival of around 12 months [17]. Ferroptosis, a freshly discovered subtype of nonapoptotic cell death, relates to overgeneration of iron-dependent ROS, ferroptosis can be activated in cancer cells by natural stimuli and synthetic agent [3]. Some small molecules could induce ferroptosis in various tumor cells, such as GC [6], fibrosarcoma [18], kidney cancer [19] and prostate cancer cells [20].

Nrf2 is a transcription factor that initiates some transcriptions to safeguard cells from endogenous or exogenous injuries, such as oxidative stress and xenobiotic, via activating cellular antioxidant response [21]. Overexpression of Nrf2 has been verified in many kinds of malignant tumors, such as breast, ovarian, and pancreatic cancers. In our experiment, we detected the expression of Nrf2 in 50 cases of gastric cancer samples by qPCR, compared to the precancerous tissues; Nrf2 mRNA was highly expressed in cancer samples. Patients whose tumors exhibit higher level of Nrf2 usually present poor prognosis [22]. To reveal the influence of Nrf2 on the prognosis of gastric cancer patients, high- and low-Nrf2 expression group was divided according to expression of Nrf2 in the recruited gastric cancer specimens, and then Kaplan–Meier analyses were performed. There was prominent survival difference between Nrf2 low and Nrf2 high groups. These results indicated that Nrf2 plays an important role in occurrence and development of gastric cancer.

Constitutive activation of Nrf2-ARE shields malignant cells from oxidative damages [23, 24]. Therefore, it has recently been deemed to be a main defense mechanism and a cytoprotective transcription factor of tumor cells that are resistant to ferroptosis [11], Nrf2 overexpression rescues sorafenib-induced ferroptosis in hepatocellular carcinoma [5, 25], on the contrary, Nrf2 inhibition reverses the resistance of cisplatin-resistant neck and head cancer cells to artesunate-mediated ferroptosis [13].

Previous studies confirmed that miRNAs play an important role in the progression and development of various types of malignant tumors. miR-144 could target Nrf2 mRNA, leading to the downregulation of Nrf2 in cancer cells [14, 26]. miR-144-5p expression is downregulated in many kinds of human cancers, such as colon, liver, and bladder cancers [27]. miR-144-5p can restrain the proliferation, migration, and invasion of malignant tumor cells through many mechanisms [28]. In the experiment, we found that miR-144-5p was highly expressed in a panel of 62 cases of gastric cancer samples compared to the precancerous tissues; in addition, low expression of miR-144-5p involved in bad survival of gastric cancer patients. To reveal the influence of miR-144-5p on the biology of gastric cancer cells, gain and loss function experiment was performed. Overexpressing of miR-144-5p by transfecting a miR-144-5p mimic into GC cells inhibited the proliferation of GC cells; by contrast, anti miR-144-5p inhibitor promoted the proliferation of GC cells. Taken together, these data suggest that miR-144-5p is possibly involved in growth of gastric cancer cell and may worked as a role of tumor suppressor gene.

A meta-analysis was conducted on the basis of microarrays from the GEO database to explore the function of overexpression of miR-144-5p in malignant cell. Among the involved genes of miR-144-5p,

some genes play a role on the anti-oxidative stress of cells, such as serpin peptidase inhibitor, clade B (ovalbumin), member 5 (SERPINB5), Carbonic Anhydrase IX (CA9) and Early growth response-1 (EGR1), indicating that miR-144-5p might play an important role in the oxidative stress. In our study, we found that exogenous miR-144-5p intensified the overproduction of ROS and proliferation inhibition of GC cells, highlighting that miR-144-5p participated in oxidation reaction.

Further, with help of MiRWALK2.0, TargetScan, PICTAR2 software, the targeted genes of miR-144-5p were predicated, among the targeted genes, Nrf2 was listed. On the contrary, when Nrf2 was put in, miR-144-5p was found. In consideration of both Nrf2 and miR-144-5p are associated with oxidative stress, Nrf2 was likely a target of miR-144-5p in gastric cancer. To further test this hypothesis, dual luciferase report assay was performed, overexpression of miR-144-5p could abrogated the luciferin intensity of wild type group, but not the mutant group.

In order to detect whether miR-144-5p could enhance the sensitization of gastric cancer cell to erastin-induced ferroptosis, exogenous miR-144-5p was introduced into gastric cancer cells. Results showed that cancer cell with overexpression of miR-144-5p were more sensitive to erastin with overgeneration of ROS and depletion of GSH. Exogenous Nrf2 rescued miR-144-5p promoted ferroptosis, indicating that miR-144-5p sensitized erastin-induced ferroptosis via modulating Nrf2.

Conclusion

In conclusion, our findings demonstrate that Nrf2 plays a pivotal role in GC progression. Additionally, Nrf2 activation is associated with resistance to erastin-induced ferroptosis. miR-144-5p could sensitize erastin-induced ferroptosis by wrecking Nrf2 mRNA. Thus, Nrf2 may be a promising molecular target for enhancement of erastin-induced ferroptosis in the context of oxidative stress.

Declarations

Acknowledgements

Not applicable.

Authors' contributions

RH devoted to research design and data curations. CL, WD and LL were responsible for experiment and figures. All authors read and approved the final manuscript.

Funding

None.

Availability of data and materials

All data generated or analyzed during this study are included in this published article.

Ethics approval and consent to participate

A total of 50 patients with gastric cancer who had not received any chemotherapy and radiotherapy before surgery were recruited from t Weifang People's Hospital. The procedures of the human experiments was authorized by Medical Ethics Committee of Weifang People's Hospital. In addition, all involved participants signed informed consent.

Consent for publication

All authors have approved the publication of this manuscript.

Competing interests

The authors declare that they have no competing interests.

References

1. Forcina GC, Dixon SJ. GPX4 at the Crossroads of Lipid Homeostasis and Ferroptosis. Proteomics. 2019:e1800311.
2. Gai C, Yu M, Li Z, Wang Y, Ding D, Zheng J, Lv S, Zhang W, Li W. Acetaminophen sensitizing erastin-induced ferroptosis via modulation of Nrf2/heme oxygenase-1 signaling pathway in non-small-cell lung cancer. J Cell Physiol. 2020;235(4):3329–39.
3. Dixon SJ, Lemberg KM, Lamprecht MR, Skouta R, Zaitsev EM, Gleason CE, Patel DN, Bauer AJ, Cantley AM, Yang WS, et al. Ferroptosis: an iron-dependent form of nonapoptotic cell death. Cell. 2012;149(5):1060–72.
4. Zhang W, Gai C, Ding D, Wang F, Li W. Targeted p53 on Small-Molecules-Induced Ferroptosis in Cancers. Front Oncol. 2018;8:507.
5. Xie Y, Hou W, Song X, Yu Y, Huang J, Sun X, Kang R, Tang D. Ferroptosis: process and function. Cell Death Differ. 2016;23(3):369–79.
6. Hao S, Yu J, He W, Huang Q, Zhao Y, Liang B, Zhang S, Wen Z, Dong S, Rao J, et al. Cysteine Dioxygenase 1 Mediates Erastin-Induced Ferroptosis in Human Gastric Cancer Cells. Neoplasia. 2017;19(12):1022–32.
7. Yagoda N, von Rechenberg M, Zaganjor E, Bauer AJ, Yang WS, Fridman DJ, Wolpaw AJ, Smukste I, Peltier JM, Boniface JJ, et al. RAS-RAF-MEK-dependent oxidative cell death involving voltage-dependent anion channels. Nature. 2007;447(7146):864–8.
8. Rojo de la. Vega M1, Chapman E1, Zhang DD2. NRF2 and the Hallmarks of Cancer. Cancer Cell. 2018 Jul 9;34(1):21–43.
9. Kawasaki Y, Ishigami S, Arigami T, Uenosono Y, Yanagita S, Uchikado Y, Kita Y, Nishizono Y, Okumura H, Nakajo A, et al. Clinicopathological significance of nuclear factor (erythroid-2)-related factor 2

(Nrf2) expression in gastric cancer. BMC Cancer. 2015;15:5.
10. Sajadimajd S, Khazaei M. Oxidative Stress and Cancer. The Role of Nrf2. Curr Cancer Drug Targets. 2018;18(6):538–57.
11. Dodson M, Castro-Portuguez R, Zhang DD. NRF2 plays a critical role in mitigating lipid peroxidation and ferroptosis. Redox Biol. 2019:101107.
12. Shin D, Kim EH, Lee J, Roh JL. Nrf2 inhibition reverses resistance to GPX4 inhibitor-induced ferroptosis in head and neck cancer. Free Radic Biol Med. 2018;129:454–62.
13. Roh JL, Kim EH, Jang H, Shin D. Nrf2 inhibition reverses the resistance of cisplatin-resistant head and neck cancer cells to artesunate-induced ferroptosis. Redox Biol. 2017;11:254–62.
14. Yan Y, Gong Z, Xu Z. Commentary. Lico A causes ER stress and apoptosis via up-regulating miR-144-3p in human lung cancer cell line H292. Biomed J. 2018;41(6):391–2.
15. Sun X, Liu D, Xue Y, Hu X. Enforced miR-144-3p Expression as a Non-Invasive Biomarker for the Acute Myeloid Leukemia Patients Mainly by Targeting NRF2. Clin Lab. 2017;63(4):679–87.
16. Coelho RC, Abreu PDP, Monteiro MR, Stramosk AP, Garces AHI, Melo AC, Graudenz MS, Andrade CJC. Cisplatin, Fluorouracil in Bolus Injection, and Leucovorin in First-Line Therapy for Advanced Gastric Cancer as an Alternative to Protocols With Infusional Fluorouracil. J Glob Oncol. 2019;5:1–8.
17. Taieb J, Moehler M, Boku N, Ajani JA, Yanez Ruiz E, Ryu MH, Guenther S, Chand V, Bang YJ. Evolution of checkpoint inhibitors for the treatment of metastatic gastric cancers: Current status and future perspectives. Cancer Treat Rev. 2018;66:104–13.
18. Shintoku R, Takigawa Y, Yamada K, Kubota C, Yoshimoto Y, Takeuchi T, Koshiishi I, Torii S. Lipoxygenase-mediated generation of lipid peroxides enhances ferroptosis induced by erastin and RSL3. Cancer Sci. 2017;108(11):2187–94.
19. Kerins MJ, Milligan J, Wohlschlegel JA, Ooi A. Fumarate hydratase inactivation in hereditary leiomyomatosis and renal cell cancer is synthetic lethal with ferroptosis induction. Cancer Sci. 2018;109(9):2757–66.
20. Tang M, Chen Z, Wu D, Chen L. Ferritinophagy/ferroptosis. Iron-related newcomers in human diseases. J Cell Physiol. 2018;233(12):9179–90.
21. Dodson M, de la Vega MR, Cholanians AB, Schmidlin CJ, Chapman E, Zhang DD. Modulating NRF2 in Disease. Timing Is Everything. Annu Rev Pharmacol Toxicol. 2019;59:555–75.
22. Namani A, Matiur Rahaman M, Chen M, Tang X. Gene-expression signature regulated by the KEAP1-NRF2-CUL3 axis is associated with a poor prognosis in head and neck squamous cell cancer. BMC Cancer. 2018;18(1):46.
23. Sporn MB, Liby KT. NRF2 and cancer. the good, the bad and the importance of context. Nat Rev Cancer. 2012;12(8):564–71.
24. Lu K, Alcivar AL, Ma J, Foo TK, Zywea S, Mahdi A, Huo Y, Kensler TW, Gatza ML, Xia B. NRF2 Induction Supporting Breast Cancer Cell Survival Is Enabled by Oxidative Stress-Induced DPP3-KEAP1 Interaction. Cancer Res. 2017;77(11):2881–92.

25. Tuo L, Xiang J, Pan X, Gao Q, Zhang G, Yang Y, Liang L, Xia J, Wang K, Tang N. PCK1 Downregulation Promotes TXNRD1 Expression and Hepatoma Cell Growth via the Nrf2/Keap1 Pathway. Front Oncol. 2018;8:611.
26. Jadeja RN, Jones MA, Abdelrahman AA, Powell FL, Thounaojam MC, Gutsaeva D, Bartoli M, Martin PM. Inhibiting microRNA-144 potentiates Nrf2-dependent antioxidant signaling in RPE and protects against oxidative stress-induced outer retinal degeneration. Redox Biol. 2020;28:101336.
27. Gao Z, Zhang P, Xie M, Gao H, Yin L, Liu R. miR-144/451 cluster plays an oncogenic role in esophageal cancer by inhibiting cell invasion. Cancer Cell Int. 2018;18:184.
28. Li J, Sun P, Yue Z, Zhang D, You K, Wang J. miR-144-3p Induces Cell Cycle Arrest and Apoptosis in Pancreatic Cancer Cells by Targeting Proline-Rich Protein 11 Expression via the Mitogen-Activated Protein Kinase Signaling Pathway. DNA Cell Biol. 2017;36(8):619–26.

Figures

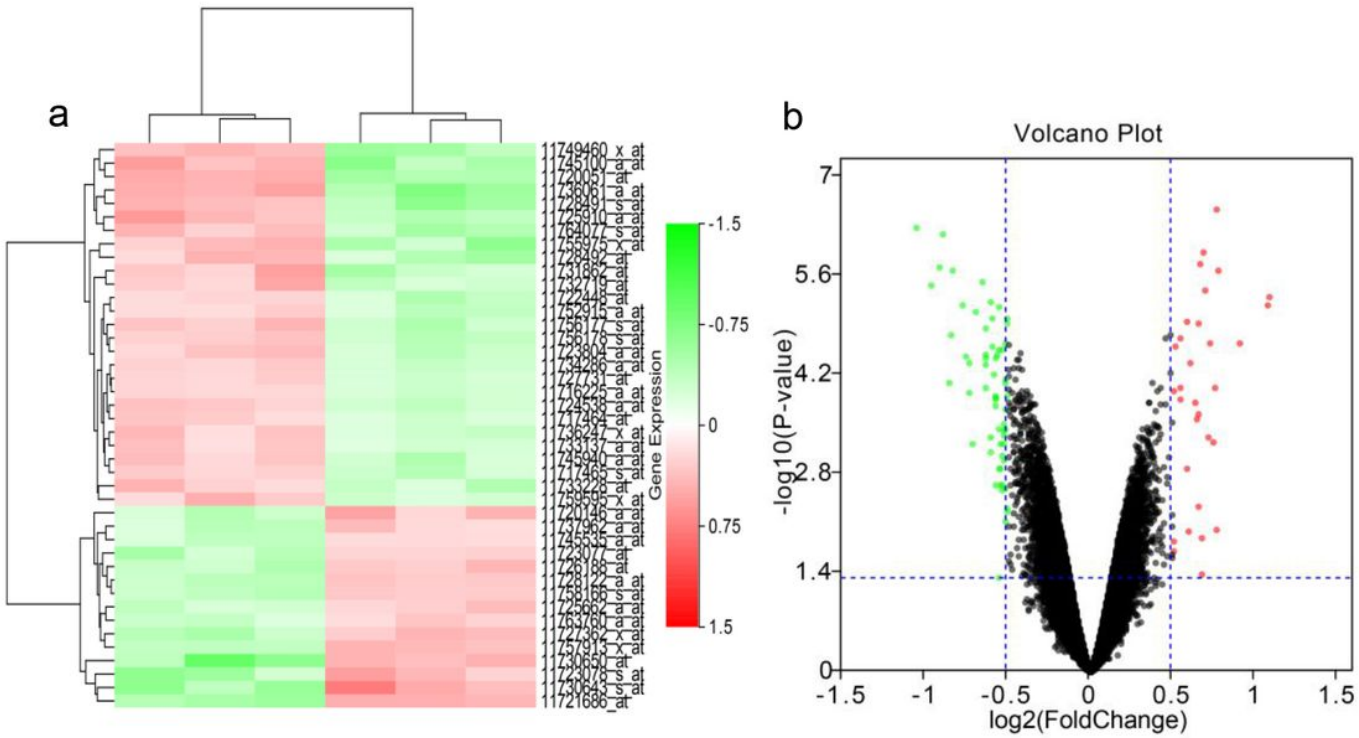

Figure 1

MiR-144-5p involved in oxidized injury through GEO Microarrays (a) Hotmap of differences in gene expression when miR-144-5p was overexpressed. (b) Volcano plot of differences in gene expression when miR-144-5p was overexpressed.

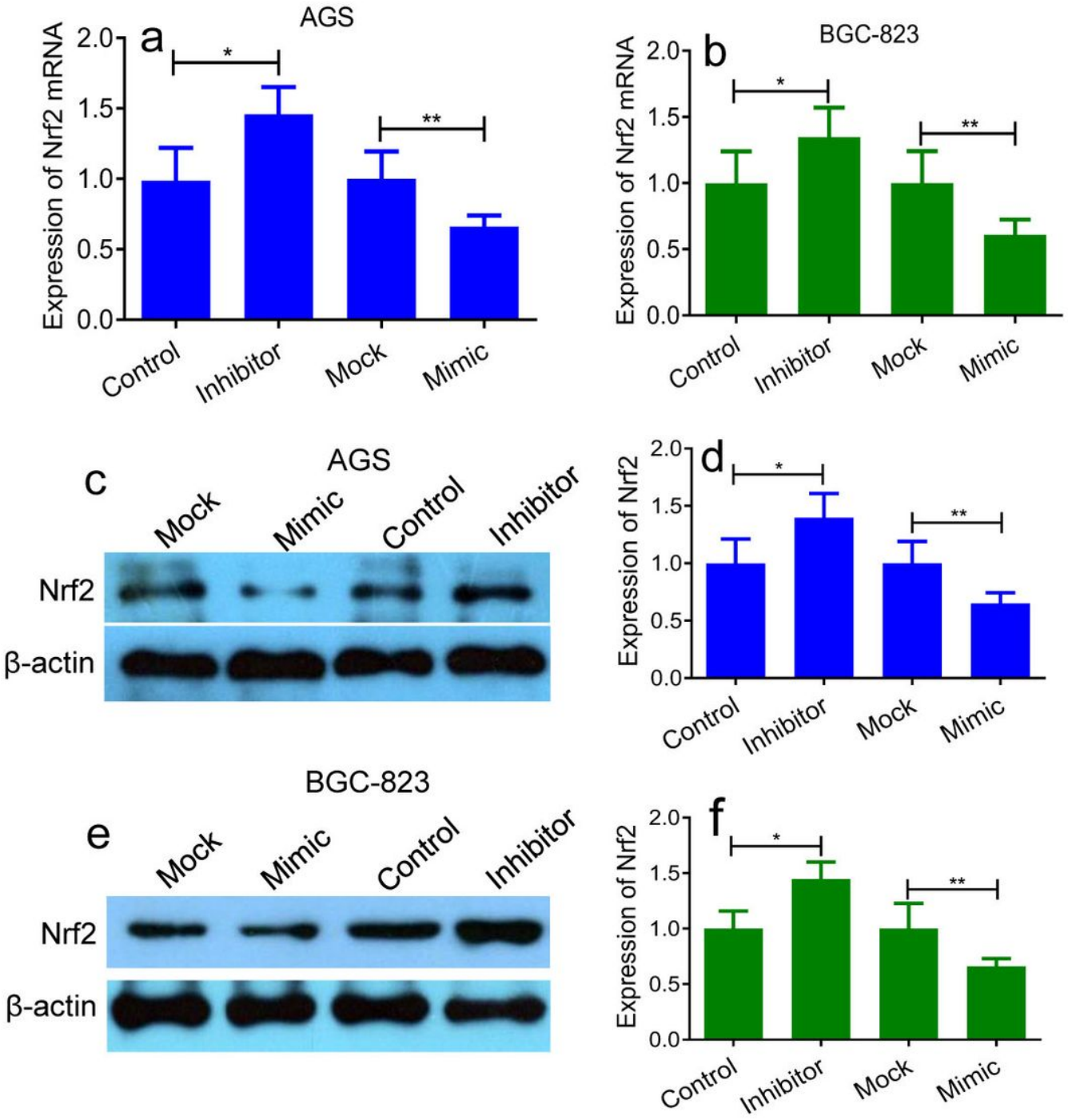

Figure 2

miR-144-5p impaired expression of Nrf2 in GC cells (a, b) qPCR analysis of Nrf2 mRNA regulated by miR-144-5p mimic or miR-144-5p inhibitor in AGS and BGC-823 cells. (c-f) Western blot analysis of Nrf2 protein regulated by miR-144-5p mimic or miR-144-5p inhibitor in AGS and BGC-823cells. *P < 0.05, ** P < 0.01.

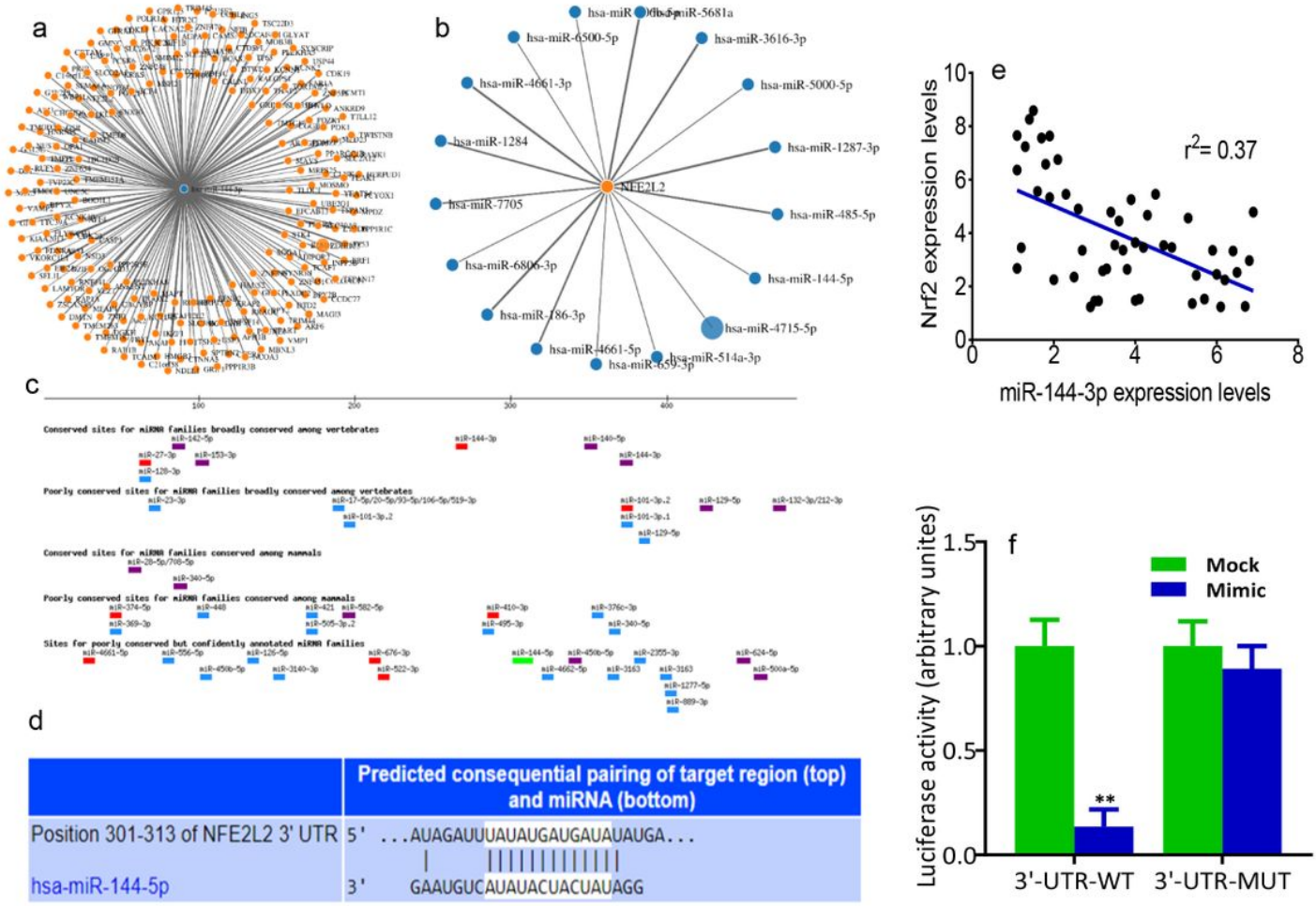

Figure 3

Nrf2 is a potent target of miR-144-5p (a) Potent targeted genes of miR-144-5p analyzed by miRWalk. (b) Latent miRNAs targeting Nrf2. (c, d) The targeted site and sequence of miR-144-5p on Nrf2. (e) miR-144-5p was inversely correlated with Nrf2 expression in gastric cancer tissues (r2=0.47). (f) Overexpression of miR-144-5p suppressed Nrf2 3'-UTR luciferase activity, but cannot suppressed luciferase activity with mutant Nrf2 3'-UTR.

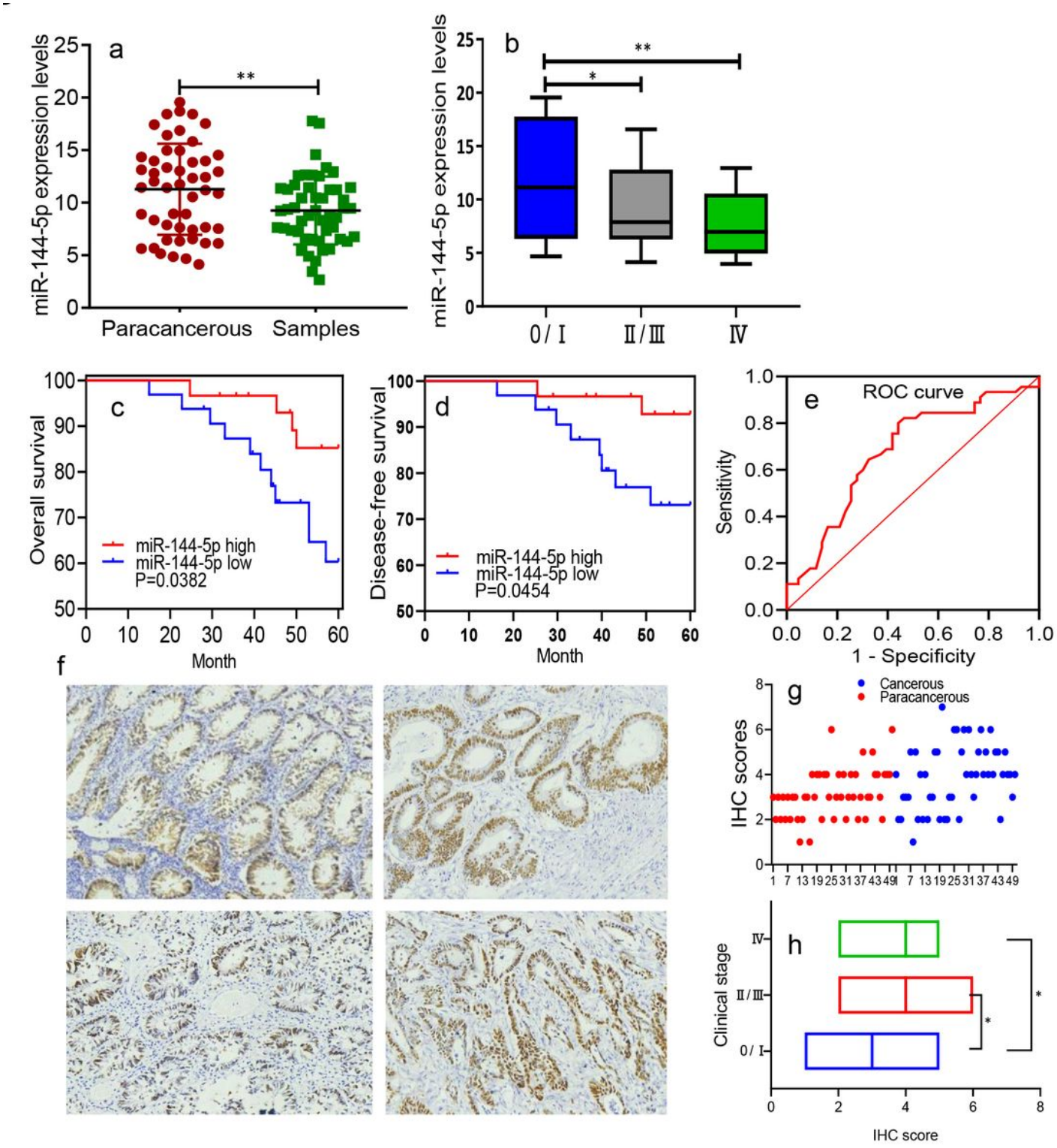

Figure 4

Association of miR-144-5p and Nrf2 with clinicopathological features (a) Expression of miR-144-5p in gastric cancer sample was quantitatively analyzed using qPCR and normalized with U6 snRNA. (b) Validation of miR-144-5p in gastric cancer specimens with different clinical stages. (c) Correlations between the miR-144-5p expression and disease-free survival of breast cancer patients s. (d) Kaplan-Meier analyses of correlations between the miR-144-5p expression level and overall survival of breast

cancer patients. (e) ROC curve of PVT1 for differentiating breast cancer patients from healthy individuals. (f) Expression of Nrf2 in gastric cancer tissue and paracancerous tissue, left up: paracancerous tissue; left low: low expression of Nrf2 in gastric cancer tissue; right up: medium expression of Nrf2 in gastric cancer tissue; right low: high expression of Nrf2 in gastric cancer tissue. (g) High expression of Nrf2 in gastric cancer tissues. (h) Intensive Nrf2 expression in high clinical stage of gastric cancer.

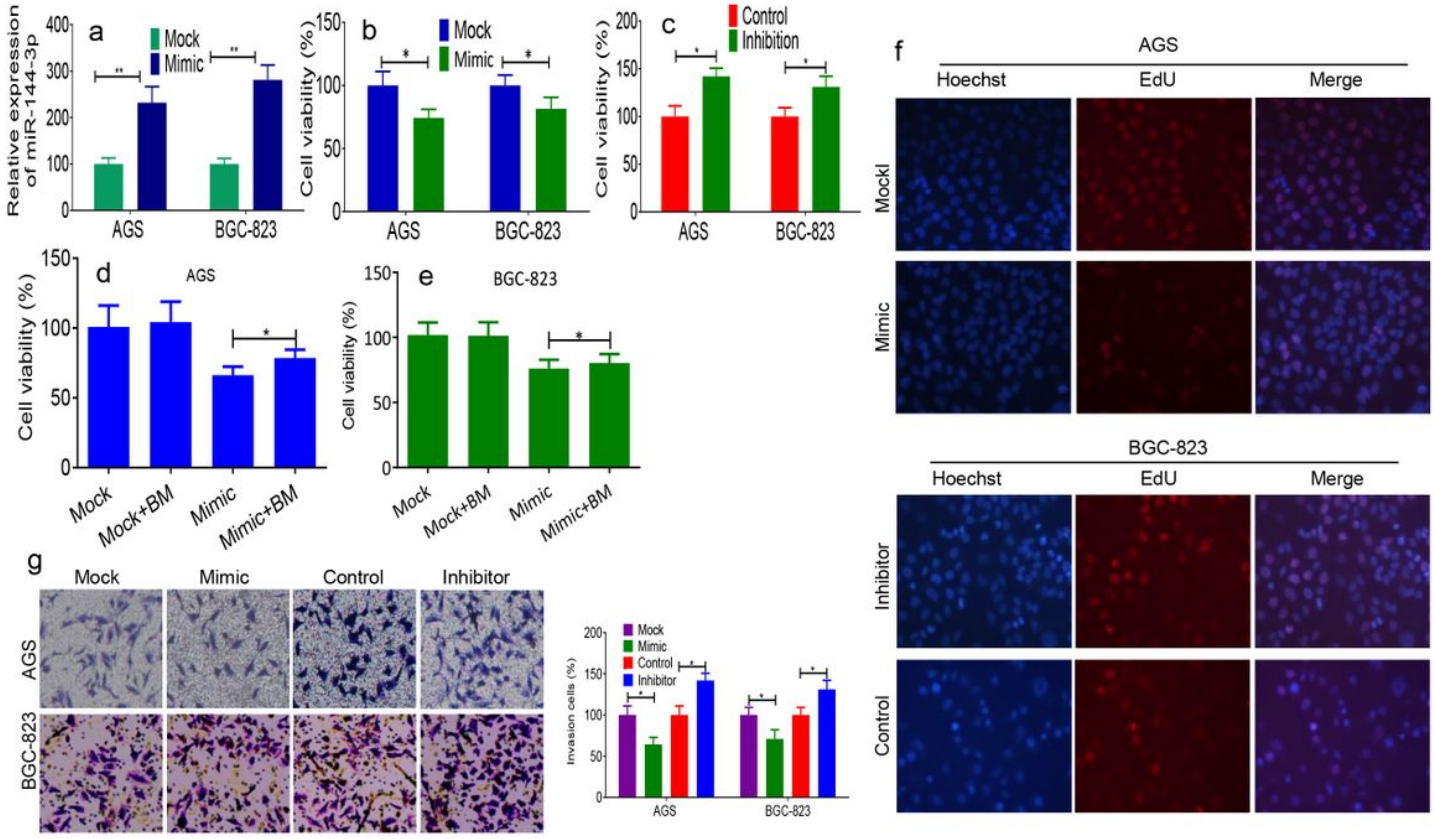

Figure 5

miR-144-5p inhibited cell viability and invasion in GC cells (a) miR-144-5p mimic led to ectopic expression of miR-144-5p in AGS and BGC-823 cells, disordered 21nt RNA was transfected as mock group. (b) Exogenous expression of miR-144-5p suppressed proliferation of AGS and BGC-823 cells. (c) Inhibition of miR-144-5p promoted cell proliferation. (d, e) MTT assay revealed protection of exogenous Nrf2 against miR-144-5p in AGC cell and BGC-823 cells. (f) Ectopic expression miR-144-5p inhibited cell proliferation that was further confirmed by EdU assay. (g) Inhibition of miR-144-5p promoted GC cell invasion, and miR-144-5p mimic augmented cell invasive ability as determined by a transwell assay. *P < 0.05, ** P < 0.01.

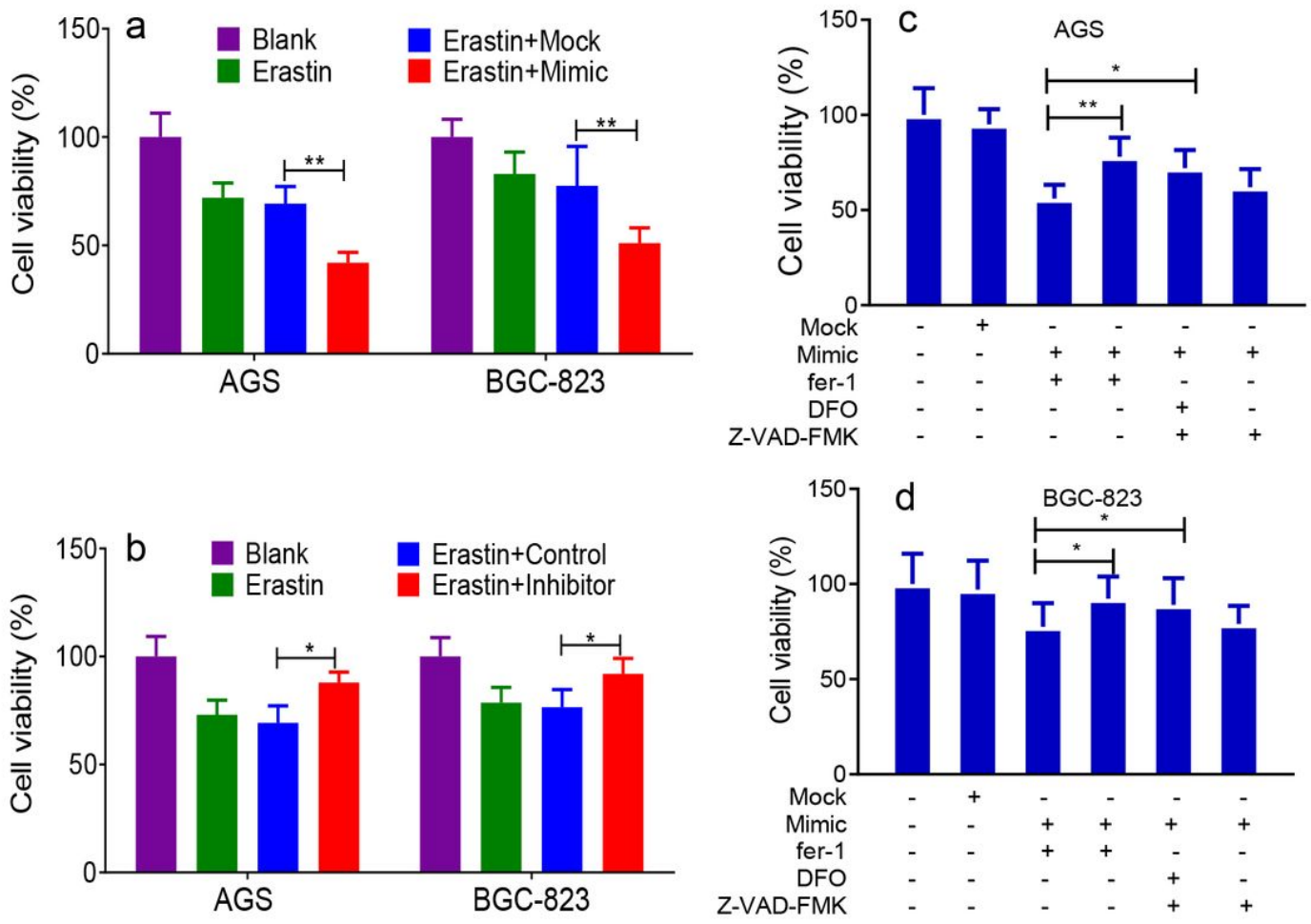

Figure 6

miR-144-5p sensitized erastin-induced ferroptosis in GC cells (a) Ectopic expression of miR-144-5p enhanced erastin-induced inhibition of proliferation in A549 cell confirmed by MTT. (b) Inhibition of miR-144-5p rescued erastin-induced inhibition of proliferation confirmed by MTT. (c, d) DFO or ferrostatin-1 effectively inhibited miR-144-5p induced inhibition of cell proliferation in AGC cell and BGC-823 cell, respectively. *P < 0.05, ** P < 0.01.

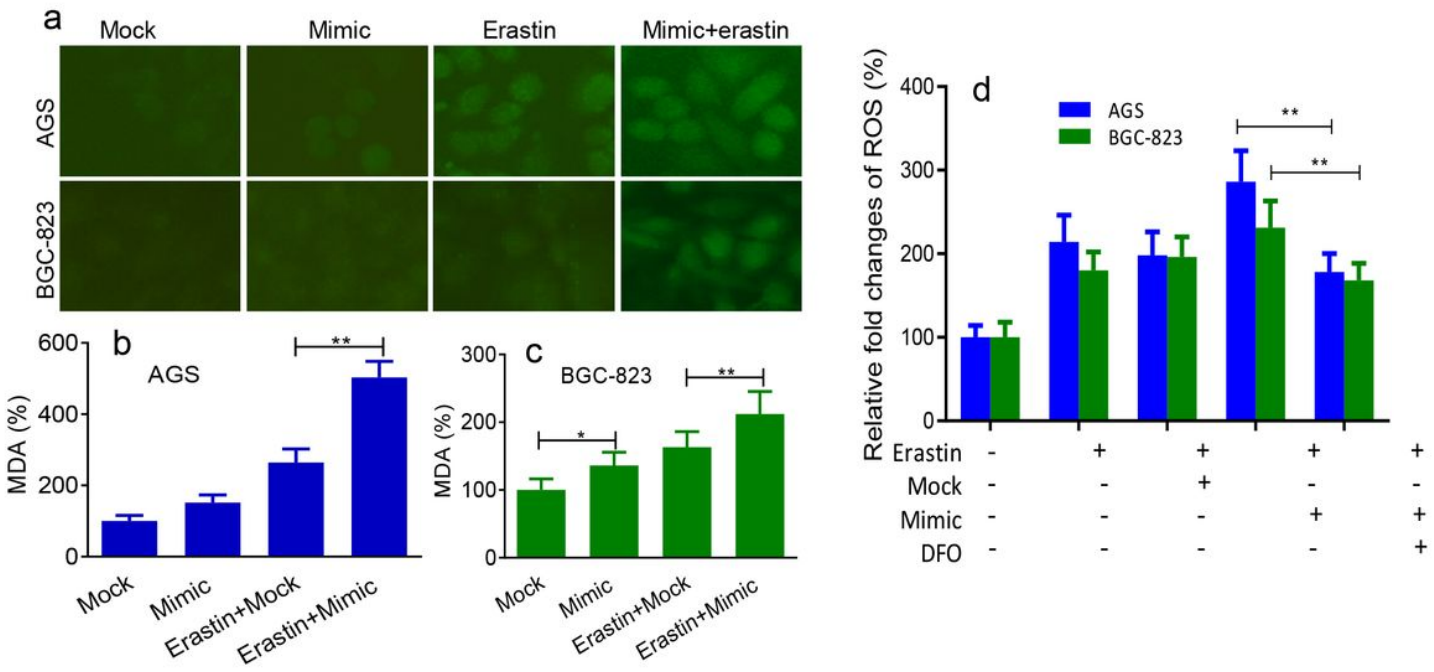

Figure 7

miR-144-5p enhanced erastin-induced overgeneration of lipid oxidation (a) miR-144-5p mimic augmented erastin-induced increase of ROS as detected by DCFH-DA. (b, c) miR-144-5p mimic and erastin led to increase of MDA in AGC and BGC-823 cells, respectively. (d) AGS and BGC-823 cells were treated with erastin in the absence or presence of miR-144-5p inhibitor for 8 h and ROS was measured by DCFH-DA. *P < 0.05, ** P < 0.01.

Supplementary Files

This is a list of supplementary files associated with this preprint. Click to download.

- supplementalTable1.xlsx
- supplementalTable2.xlsx
- supplementalTable3.xlsx